EAI Endorsed Transactions
on Energy Web
Research Article EAI.EU

A novel dung beetle optimization algorithm of distribution network reconfiguration for power loss reduction and reliability improvement

Yanmin Wu[1], Ruiliang Guo[1], Lu Wang[2,*], Xiangqian Zhu[1] and Zhenjie Wan[1]

[1]Zhengzhou University of Light Industry, Zhengzhou 450002, China
[2]Hohai University, Nanjing 211100, China

Abstract

In the evolution of energy systems, investigations into distribution networks have concentrated on enhancing reliability and optimizing performance. Distribution networks with distributed energy resources are expected to significantly enhance power accommodation capacity, but load flow distribution and network optimization remain key challenges. This study aims to develop an improved dung beetle optimization (IDBO) algorithm to minimize active power losses and node voltage deviations in distribution networks, while validating its superiority over existing algorithms across different network configurations. The IDBO algorithm is enhanced through three key strategies: (i) A variable spiral search strategy is employed to improve search efficiency and global exploration. (ii) A levy flight strategy is introduced to prevent algorithm premature convergence. (iii) A t-distribution adjustment strategy based on iteration count is adopted to strengthen local search capability. To verify whether the IDBO algorithm can achieve the optimal load flow distribution that meets the reliability requirements of distribution network operation, relevant validations have been conducted. Experimental results demonstrate that IDBO achieves faster convergence and superior performance on classical test functions. In practical applications to IEEE 33-bus and 69-bus distribution systems, it significantly reduces power losses and improves voltage profiles compared to other algorithms. The proposed IDBO algorithm provides an effective solution for distribution network reconfiguration, demonstrating enhanced optimization capability, improved convergence characteristics, and reliable performance across various operating conditions.

Keywords: distribution network reconfiguration, artificial intelligence algorithm, IDBO algorithm, distributed generation

Received on 5 October 2025, accepted on 16 November 2025, published on 09 February 2026

doi: 10.4108/ew.11841

1. Introduction

To achieve secure and reliable power supply and facilitate a clean low-carbon transition, further enhancement and upgrading of the distribution network are necessary. On March 1, 2024, the National Development and Reform Commission and the National Energy Administration[1] issued the "Guiding Opinions on the High-Quality Development of Distribution Networks in the New Situation," proposing the establishment of a novel type of distribution system that was safe, efficient, clean, low-carbon, flexible, adaptive, and intelligent. [2] The incorporation of renewable energy sources significantly enhances the supply capacity, distribution capacity, resilience, and flexibility of the new distribution system. However, instability poses a key obstacle limiting its widespread application[3]. In this context, optimizing and restructuring distribution networks have become the mainstream trend to support the transformation of the grid. [4]

Distribution network reconfiguration (DNR) involves optimizing the flow paths of electric currents, thereby

*Corresponding author. Email: 332413030872@email.zzuli.edu.cn

improving the performance and reliability of the grid. [5] Losses in distribution networks primarily arise from the resistance and reactance encountered by electric currents during transmission, which lead to energy conversion into heat and subsequent loss. Measures such as restructuring network topology and integrating distributed energy resources can effectively reduce the losses of energy caused by resistance and reactance. By DNR and careful consideration of the locations and capacities of distributed energy resource connections, not only can power supply reliability be enhanced, but it can also contribute to promote the widespread application of clean energy, which can serve as a good corresponding to the "dual carbon" objectives. [6]

In DNR, the objective functions and constraints often involve nonlinear power flow equations, power balance equations, which are typically non-convex. Furthermore, the inclusion of discrete and integer variables in distribution network problems further exacerbates the non-convex nature of the problem. This discretization and non-convexity make the DNR problem more closely aligned with the practical functioning of power systems, thereby adding intricacy and challenge to the issue. To address this issue, traditional mathematical methods, heuristic algorithms, and artificial intelligence algorithms can be employed. These methods can effectively optimize the DNR's results, enhancing system efficiency and stability. By reviewing the literature, it was discovered that when a problem has a very large exploration space or it is challenging to establish precise mathematical models, traditional mathematical algorithms reveal the drawback of low computational efficiency. And the heuristic algorithms in current literature cannot guarantee finding the global optimal solution and may sometimes converge to local optima. In contrast, artificial intelligence algorithms are evolving towards increased adaptability, integrating the strengths of multiple heuristic algorithms to enhance algorithm robustness and search capabilities. Ref. [7] provided a detailed explanation of the Dragonfly Algorithm (DA), elucidating its principles of separation, alignment, cohesion, attraction, and distraction, then simulated on an enhanced IEEE 16-bus network to validate its effectiveness in losses reduction and network performance enhancement. Ref. [8] devised switching functions incorporating instantaneous operational cost variations and integrates a trained LSTM model for grid reconfiguration. Case studies showcase the effectiveness and robustness of this approach. Ref. [9] introduced a multi-objective approach which considered both the aggregate active power losses and the comprehensive network voltage stability. The optimization function was assessed using load flow methods, and the proposed Enhanced Sine-Cosine Algorithm (ESCA) was benchmarked against other established algorithms, showcasing its superiority. Ref. [10] applied the Harris Hawks Optimization (HHO) to solve optimization issues and successfully minimizes total network losses by 21.428% in a case study on an 83-node distribution system. In aiming to reduce active power losses, enhance voltage magnitude, and improve reliability metrics, Ref. [11] contrasted Evolutionary Optimization (EO) with ten alternative meta-heuristic search methods when tackling the reconfiguration issue in four distinct distribution test systems. Ref. [12] introduced a novel DNR method to enhance reliability metrics and lower operational costs. It applies an Improved Genetic Algorithm (IGA) to address the nonlinearity of the issue and decrease computation time. Ref. [13] discussed DNR considering electric vehicles and DGs, and proposed a hybrid algorithm named IPSO-ABCO to tackle the complexity of the optimization issue. These researches on DNR using meta-heuristic algorithms mentioned above have certain limitations, including insufficient global search capability, poor convergence or limited universality.

To address the shortcomings identified in the previous research, this study considers minimizing active power dissipation and reducing node voltage deviations as objective functions. It introduces adaptive parameters and applies variable spiral search strategy, levy flight strategy, and t-distribution variation based on the number of iterations to optimize and enhance the DBO. To validate the algorithm's universality more effectively, variations in the type, parameters, locations, and quantities of the connected DG units are made, and validation is conducted on the IEEE 33-bus and IEEE 69-bus systems. The primary contributions of this study are as follows:

- Proposing the IDBO algorithm to tackle DNR problem.
- Performing experiments on two distribution network configurations, IEEE 33-bus and IEEE 69-bus, to confirm the algorithm's applicability across different setups.
- Comparing the DNR results with other algorithms to verify the algorithm's performance.

In this study, the second part of paper introduces the model of DNR. In the third part, the IDBO algorithm is proposed and its performance is tested. The fourth part discusses the experimental setup and results. The fifth part summarizes the results of current research.

2. Problem definition

2.1. Objective function

Reducing active power losses[14] and voltage deviations[15,16] not only enhances the efficiency and stability of distribution networks but also lowers operational costs while ensuring user electricity demands are met. Based on this, in the process of DNR, this study sets these two objective functions.

$$\begin{cases} \min f_1 = P_{loss} = \sum_{n=1}^{N} R_n \dfrac{P_n^2 + Q_n^2}{V_n^2} \\ \min f_2 = V_{dev} = \min \sum_{i=1}^{M} \left| \dfrac{V_i - V_N}{V_N} \right| \end{cases} \tag{1}$$

Where, P_{loss}, R_n and N is the active power dissipation, resistance of n-th branch, and total number of branches,

respectively. V_n, P_n, and Q_n represent the voltage level, active power, and reactive power at the end of the n-th branch. V_{dev} and M represent voltage deviation and sum of all nodes. V_i and V_N denote the voltage level at i-th node and the reference voltage.

2.2. Constraints

To ensure the feasibility of the optimization scheme and align with actual operation needs, voltage constraints, current constraints, DG output constraints, branch capacity constraints, operation constraints, and power flow balancing constraints are introduced into the DNR model. [17,18]

$$V_{i,\min} \le V_i \le V_{i,\max} \tag{2}$$

$$I_{n,\min} \le I_n \le I_{n,\max} \tag{3}$$

$$\begin{cases} P_{DG,\min} \le P_{DG,i} \le P_{DG,\max} \\ Q_{DG,\min} \le Q_{DG,i} \le Q_{DG,\max} \end{cases} \tag{4}$$

$$S_n \le S_{n,\max} \tag{5}$$

$$g \in G \tag{6}$$

$$\begin{cases} P_i + P_{\mathrm{DG}i} = P_{Li} + V_i \sum_{j=1}^{M} V_j (G_{ij} \cos\theta_{ij} + B_{ij} \sin\theta_{ij}) \\ Q_i + Q_{\mathrm{DG}i} = \mathrm{Q}_{Li} + V_i \sum_{j=1}^{M} V_j (G_{ij} \sin\theta_{ij} - B_{ij} \cos\theta_{ij}) \end{cases} \tag{7}$$

Equation (2) indicates that the voltage V_i at i-th node is constrained within the range of $V_{i,min}$ and $V_{i,max}$; Equation (3) specifies that the current I_n flowing through n-th branch is constrained within the range of $I_{n,min}$ and $I_{n,max}$; Equation (4) constrains the DG output power $P_{DG,i}$ and $Q_{DG,i}$ at i-th node within the ranges of $P_{DG,min}$, $Q_{DG,min}$ and $P_{DG,max}$, $Q_{DG,max}$ respectively; Equation (5) ensures that the capacity S_n of n-th branch does not exceed $S_{n,max}$; In Equation (6), g represents the reconfigured structure, and G denotes the set of all feasible topologies; In Equation (7): P_i and Q_i is the active and reactive power; P_{DGi} and P_{Li} is the active power of DG and load injection at i-th node, respectively; Q_{DGi} and Q_{Li} represent the reactive power of DG and load injection at i-th node, respectively; G_{ij}, B_{ij} and θ denotes the conductance, susceptance and impedance angle between i-th node and j-th node.

3. Algorithm improvements

3.1. DBO algorithm

The design of DBO algorithm draws inspiration from the rolling behavior of dung beetles[19]. The algorithmic population comprises four types of individuals performing distinct roles: rolling beetles, breeding beetles, larvae beetles, and thief beetles, with population ratios of 6:6:7:11. During algorithm iterations, the position of the rolling beetles are updated according to Equation (8) [20].

$$X_i(t+1) = X_i(t) + \alpha k X_i(t-1) + b\left|X_i(t) - X^W(t)\right| \tag{8}$$

$$\lambda = 0.1, \eta = rand(1), \begin{cases} \eta > \lambda & \alpha = 1 \\ \eta < \lambda & \alpha = -1 \end{cases} \tag{9}$$

Where, i = 1, 2, 3, … , NP; The position of individual i within the population at iteration t is denoted by $X_i(t)$. The value of the direction control parameter α is jointly determined by constant λ and a random variable η. When $\alpha = 1$, the individual moves along the intended direction. When $\alpha = -1$, it signifies adeviation from the original path. The parameter $k \in (0, 0.2]$ controls the magnitude of deviation, $b \in (0,1)$ is a natural coefficient, and $X^W(t)$ denotes the position with the poorest fitness value in the entire population.

When roling beetles encounters an obstacle during its movement, its position is updated according to Equation (10):

$$X_i(t+1) = X_i(t) + \tan\theta\left|X_i(t) - X_i(t-1)\right| \tag{10}$$

Where, $\theta \in [0, \pi]$ .The spawning boundary for the breeding beetle and the subsequent update of the egg's position are determined by Equation (11) to (13):

$$Lb^* = \max\left\{X_i^* \times \left[1 - \left(1 - t/T_{\max}\right)\right], Lb\right\} \tag{11}$$

$$Ub^* = \max\left\{X_i^* \times \left[1 - \left(1 - t/T_{\max}\right)\right], Ub\right\} \tag{11}$$

$$B_i(t+1) = X_i^* + b_1(B_i(t) - Lb^*) + b_2(B_i(t) - Ub^*) \tag{12}$$

Where, $Ub^*$and Lb^* define the edges of the area where eggs are laid, with X_i^* representing the position currently determined as the most favorable within this area during the search process. $T_{\max}$ represents the maximum number of iterations, while Ub and Lb denote the upper and lower bounds of the optimization problem, $B_i(t)$ represents the position information of the i-th egg at iteration t, $b_1$and b_2 are two mutually independent vectors, each with a norm of $1\times D$, where D represents the dimension.

The positions of larval beetles in the population also change during foraging, with their foraging behavior and optimal foraging boundaries simulated by Equation (14) to (16).

$$Lb^* = \max\left\{X_i^b \times \left[1-\left(1-t/T_{\max}\right)\right], Lb\right\} \quad (13)$$

$$Ub^* = \max\left\{X_i^b \times \left[1-\left(1-t/T_{\max}\right)\right], Ub\right\} \quad (14)$$

$$X_i(t+1) = X_i(t) + C_1(X_i(t) - Lb^b) + C_2(X_i(t) - Ub^*) \quad (15)$$

Where, X^b is the global best position. Ub^b and Lb^b define the edges of the optimal foraging area. $X_i(t)$ is the location of the i larval beetle during the t step. C_i represents a stochastic value following a normal distribution. C_i is a random value within the range (0,1).

During the iteration process, Equation (17) provides the position update formula for the dung beetle to simulate its theft behavior.

$$X_i(t+1) = X_i^b(t) + \gamma\omega\left(\left|X_i(t) - X_i^*\right| + \left|X_i(t) - X_i^b(t)\right|\right) \quad (16)$$

Where, γ is a constant, set to 1/2 in this study. A vector ω of size 1×D is initialized, and its values evolve throughout the iteration process according to a normal distribution.

3.2. IDBO algorithm

Variable spiral search strategy

In the dung beetle optimization algorithm, during the process of updating the positions of followers and discoverers, the position of the followers changes in accordance with the position of the discoverers. This results in a blind and monotonous change in the position of the followers. Professor Mirjalili from Torrens University in Australia proposed two algorithms: WOA[21] and MFO[22]. Both of these algorithms update positions using a spiral search method during the optimization process. This approach, based on prior information, adds a spiral update direction to more comprehensively search the entire problem space. It effectively improves search efficiency and avoids omissions. By integrating the variable spiral search strategy into the position update stage of breeding and foraging dung beetles[23], the original linear approach path is transformed into a spiral trajectory. This guides individuals to explore the region surrounding the optimal solution more thoroughly, effectively enhancing the algorithm's global search capability, as shown in Equation (18), where, $z = e^{k\cos(\frac{\pi l}{\max\_l})}$, L=2×$rand$−1

$$X_{i,j}^{t+1} = \begin{cases} e^{zl}\cos(2\pi l)\exp\left(\frac{X_{\text{worst}}^t - X_{i,j}^t}{i^2}\right) & i > \frac{n}{2} \\ X_P^{t+1} + \left|X_{i,j}^t - X_P^{t+1}\right| A^+ L e^{st}\cos(2\pi l) & \text{otherwise} \end{cases} \quad (17)$$

Where, the shape of the spiral search is controlled by parameter Z; k is a variable coefficient which is set to 5 in this study. l is a random number uniformly sampled from [-1, 1]. The position update formula for the modified dung beetle reproduction behavior is shown in Equation (19).

$$B_i(t+1) = X^* + e^{zl}\cos(2\pi l)b_1 C + e^{zl}\cos(2\pi l)b_2(B_i(t) - Ub^*) \quad (18)$$

The position update formula for the dung beetle foraging behavior is shown in Equation (20).

$$x_i(t+1) = e^{zl}\cos(2\pi l)x_i(t) + C_1 \times (x_i(t) - Lb^*) + C_2 \times (x_i(t) - Ub^*) \quad (19)$$

Levy flight strategy

In the DBO algorithm, the dung beetle treats the globally optimal position as its primary food source. The tendency for the entire DBO population to migrate toward the global optimum may lead to premature convergence. Incorporating the levy walk strategy characterized by its random movement into the position update mechanism simulates natural random phenomena. This enables population members to explore more extensively, avoiding local convergence while maximizing search efficiency. The step size formula is detailed in Equation (21).

$$s_i = \frac{\mu}{|\nu|^{1/\beta}} \quad (21)$$

Where, the levy flight path is denoted by s_i ; μ and v are random numbers that follow a normal distribution, μ~$N(0, \sigma_\mu^2)$, ν ~N(0, σ_ν^2). σ_μ and σ_ν are obtained from Equation (22).

$$\begin{cases} \alpha_\mu = \left\{ \dfrac{\Gamma(1+\beta)\sin(\pi\beta/2)}{\Gamma\left[(1+\beta)/2\right]2^{(\beta-1)/2}\beta} \right. \\ \sigma_\nu = 1 \end{cases} \quad (22)$$

where, Γ is the gamma coefficient, the range of values for β is 0< β <2, and in this paper β =1.

The improved position update method for the dung beetle's stealing behavior is shown in Equation (23).

$$X_i(t+1) = levy(\lambda)X_i^b(t) + \gamma\omega\left(\left|X_i(t) - X_i^*\right| + \left|X_i(t) - X_i^b(t)\right|\right) \quad (20)$$

T-distribution variation based on the number of iterations

The core of the t-distribution position perturbation strategy lies in linking the degrees of freedom parameter n of the t-distribution to the iterative process, thereby achieving adaptive variation: t-distribution perturbations are introduced as mutation operators to apply perturbations to the positions of dung beetle individuals as shown in Equation (24), achieving population variation, and updating the objective function values of the perturbed individuals. If the new value exceeds the optimal value of the previous generation, the update is executed.

$$x_i^t = x_i + x_i(iter) \quad (24)$$

Where, x_i^t is the new position of a randomly selected individual after the global t-distribution perturbation; x_i is the position before the variation; t (iter) is the value of the t-distribution, and iter is the degree of freedom in terms of the number of iterations. In the early stages of algorithm iteration, the t-distribution exhibits a flat shape resembling a Cauchy distribution, readily generating large-step perturbations that facilitate global exploration. In the later stages of iteration, the t-distribution takes on a tall shape approaching a Gaussian distribution, tending to produce small-step perturbations that enhance local exploitation. This promotes a balance between global exploration and local exploitation within the algorithm.

The algorithm flowchart for IDBO is shown in Figure 1.

3.3. Algorithm testing

To evaluate the performance of the improved dung beetle optimizer (IDBO), this study assesses its effectiveness based on 9 classic benchmark functions. By running the IDBO algorithm on test functions of varying dimensions and complexities and comparing it with the DBO, WOA, BWO[24], and SOA[25], IDBO algorithms as control group algorithms, key performance metrics including best value (BEST), average value (AVG), standard deviation (STD), and execution times (TIMES) and are set to assess their performance in convergence speed, convergence accuracy, and stability.

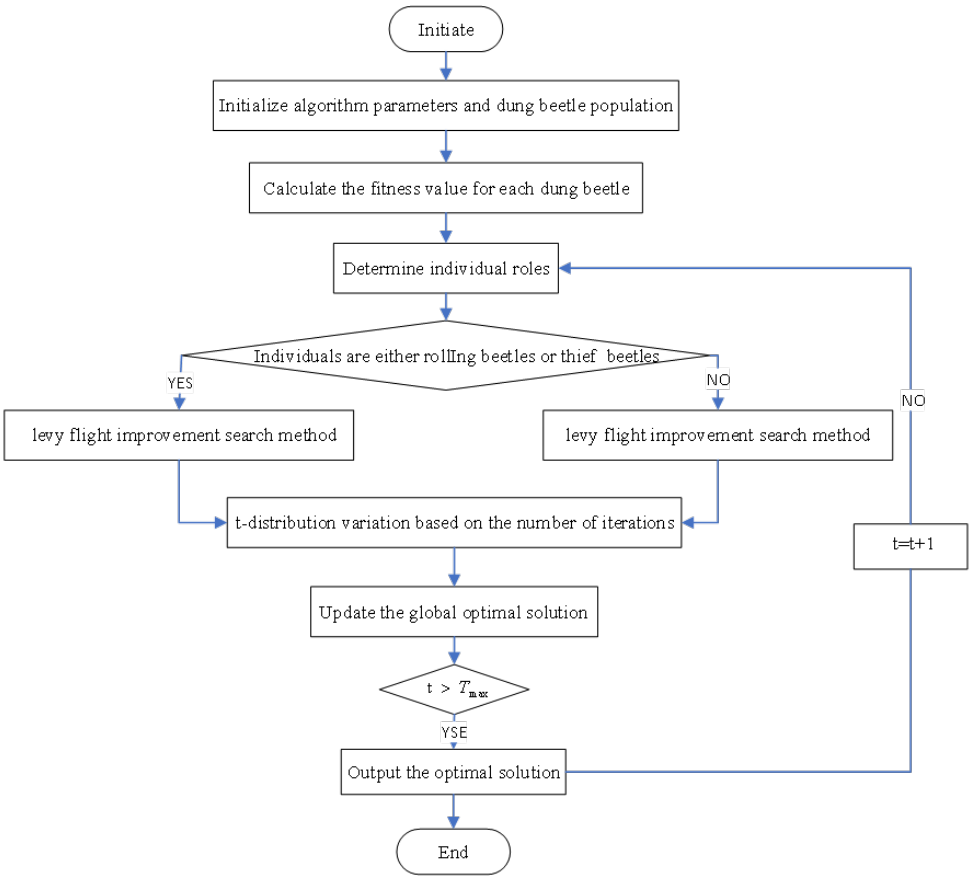

Figure 1. Flowchart for IDBO algorithm

Table 1. Algorithm settings.

Algorithm	Parament
DBO	k=0.1;b=0.3;γ=0.5
WOA	$\alpha \in (0,2)$
BWO	$H_n \in (-1,1)$
SOA	$u,v=1;f_c=2$
IDBO	k=0.1;b=0.3;γ=0.5

Table 1 summarizes the specific parameter settings employed in this study, while Table 2 provides the relevant test function formulas and parameters. Set the total population of the five algorithms to 30, run 50 cycles, each cycle iteration 500 times, the test results are shown as Table

3. Figure 2 demonstrates the convergence performance of the different algorithms on the 9 classical test functions.

As the test results in Table 3 suggest, the IDBO demonstrates faster convergence to the global optimum in terms of maximum value, while exhibiting better avoidance of local optima in terms of minimum value. Furthermore, the results of the IDBO algorithm show lower standard deviation, indicating superior stability and consistency. In Table 3, IDBO algorithm shows a stable average value, which indicates that the performance of the algorithm under different running instances is relatively consistent, indicating that the algorithm has stability. Overall, compared to DBO, WOA, BWO, and SOA, IDBO demonstrates superior optimization capabilities and higher convergence efficiency.

Based on the evaluation results of the test function, the IDBO shows satisfactory optimization ability in single-peak functions F_1 to F_4. In function F_5, IDBO is able to quickly locate the optimal solution in the feasible domain faster than other algorithms. In functions F_6 and F_7, IDBO demonstrates superior convergence speed and accuracy compared to other algorithms. In the multi-peak functions F_8 and F_9, it is evident that IDBO not only converges stably to the optimal value but also maintains the fastest convergence speed. Overall, compared to DBO, WOA, BWO, and SOA, IDBO demonstrates significant advantages in global search capability, convergence speed, and algorithmic stability.

Table 2. Test function settings

Function	Dim	Min
$F_1(x)=\sum_{i=1}^{n}x_i^2$	10	0
$F_2(x)=\sum_{i=1}^{n}([x_i+0.5])^2$	10	0
$F_3(x)=\sum_{i=1}^{n}ix_i^4+random[0,1)$	10	0
$F_4(x)=\sum_{i=1}^{n}[x_i^2-10\cos(2\pi x_i)+10]$	10	0
$F_5(x)=-20\exp(-0.2\sqrt{\frac{1}{n}\sum_{i=1}^{n}x_i^2})-\exp(\frac{1}{n}\sum_{i=1}^{n}\cos(2\pi x_i))+20+e$	10	0
$F_6(x)=F_{11}(x)=\frac{1}{4000}\sum_{i=1}^{n}x_i^2-\prod_{i=1}^{n}\cos(\frac{x_i}{\sqrt{i}})+1$	10	0
$F_7(x)=\sum_{i=1}^{11}[a_i-\frac{x_1(b_i^2+b_ix_2)}{b_i^2+b_ix_3+x_4}]^2$	4	0.0003075
$F_8(x)=-\sum_{i=1}^{5}[(x-a_i)(x-a_i)^T+c_i]^{-1}$	4	-10
$F_9(x)=-\sum_{i=1}^{10}[(x-a_i)(x-a_i)^T+c_i]^{-1}$	4	-10

Table 3. Test results

Functions	Index	WOA	SOA	BWO	DBO	IDBO
F_1	BEST	1.1854e-101	5.8131e-18	0.00e+00	4.516e-205	0.00e+00
	AVG	3.4087e-90	6.073e-15	3.2477e-310	1.28e-137	0.00e+00
	STD	1.3929e-89	1.1443e-14	0.00e+00	6.9983e-137	0.00e+00
	TIMES	0.037653	0.088075	0.13769	0.083059	0.1338
F_2	BEST	1.0512e-69	1.1649e-11	4.5512e-164	1.0731e-101	0.00e+00
	AVG	7.2165e-61	2.8274e-10	1.0171e-157	7.7335e-60	0.00e+00
	STD	2.1681e-60	2.9939e-10	4.0557e-157	4.2358e-59	0.00e+00
	TIME	0.04045	0.09347	0.14459	0.088569	0.141
F_3	BEST	9947.3829	2.6569e-09	1.3865e-307	8.548e-179	0.00e+00

	AVG	39226.5032	1.0568e-06	2.3247e-292	2.4905e-93	7.4073e-279
	STD	13625.1038	2.9547e-06	0.00e+00	1.3641e-92	0.00e+00
	TIME	0.17407	0.22529	0.28785	0.22492	0.27844
F_4	BEST	0.11727	1.0044e-05	4.9771e-160	4.499e-94	0.00e+00
	AVG	43.7452	0.0014197	2.5092e-152	6.1647e-58	0.00e+00
	STD	29.7511	0.006154	8.5014e-152	3.3766e-57	0.00e+00
	TIME	0.036718	0.087315	0.13501	0.08252	0.12937
F_5	BEST	27.0997	27.1538	24.3156	25.3093	27.5211
	AVG	27.7996	28.124	24.9757	25.6512	28.5228
	STD	0.46253	0.62569	0.22633	0.13845	0.30348
	TIME	0.058166	0.10801	0.10781	0.10735	0.16819
F_6	BEST	0.039951	2.3876	3.302	1.176e-06	1.4707e-196
	AVG	0.26382	3.0826	4.0264	0.0005111	4.5064e-17
	STD	0.16395	0.41829	0.37377	0.0016897	1.1278e-16
	TIME	0.036998	0.090157	0.13698	0.080597	0.1367
F_7	BEST	0.00012342	0.00020595	1.075e-06	0.00012587	1.238e-06
	AVG	0.0030732	0.0021828	9.4358e-05	0.00092603	0.00011875
	STD	0.0035574	0.0016	7.9564e-05	0.00072556	0.00014218
	TIME	0.11023	0.16239	0.21499	0.15509	0.20421
F_8	BEST	-12568.1468	-5916.9591	-12569.4831	-12569.4831	-12569.4866
	AVG	-10090.1123	-4943.1093	-12569.19	-8335.9099	-12569.4866
	STD	1865.4493	407.9993	0.31997	1530.9192	2.6362e-10
	TIME	0.05617	0.10744	0.17088	0.11319	0.15806
F_9	BEST	0.00e+00	0.00e+00	0.00e+00	0.00e+00	0.00e+00
	AVG	0.00e+00	0.59058	0.00e+00	1.9902	0.00e+00
	STD	0.00e+00	1.8542	0.00e+00	5.45	0.00e+00
	TIME	0.041842	0.10321	0.14443	0.090317	0.14161

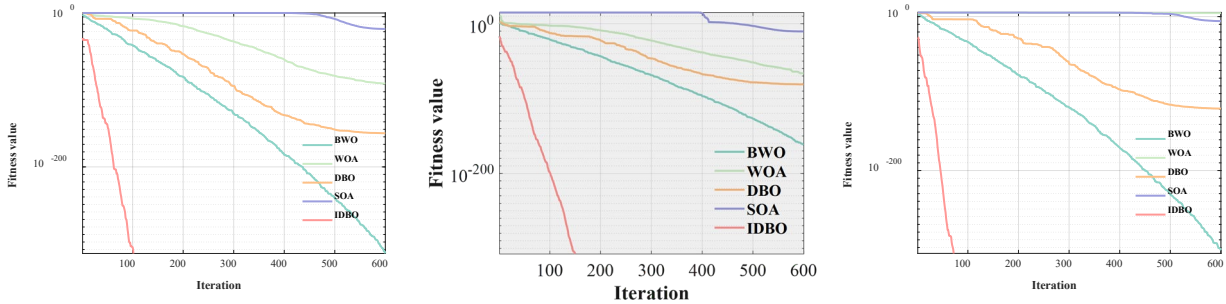

(a) F_1 (b) F_2 (c) F_3

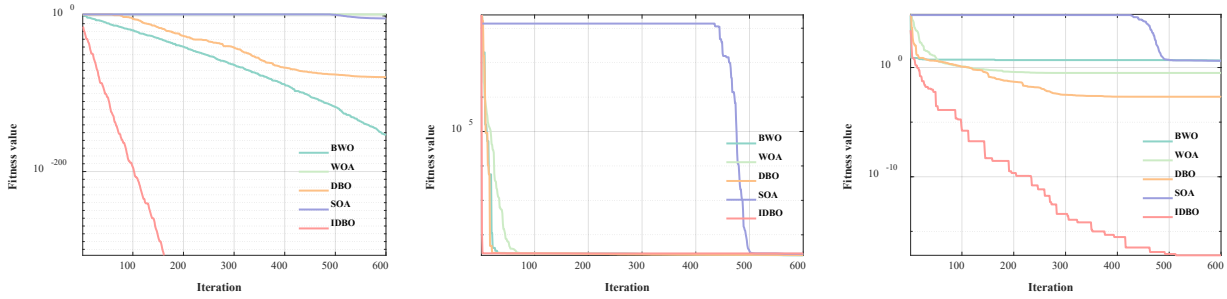

(d) F_4 (e) F_5 (f) F_6

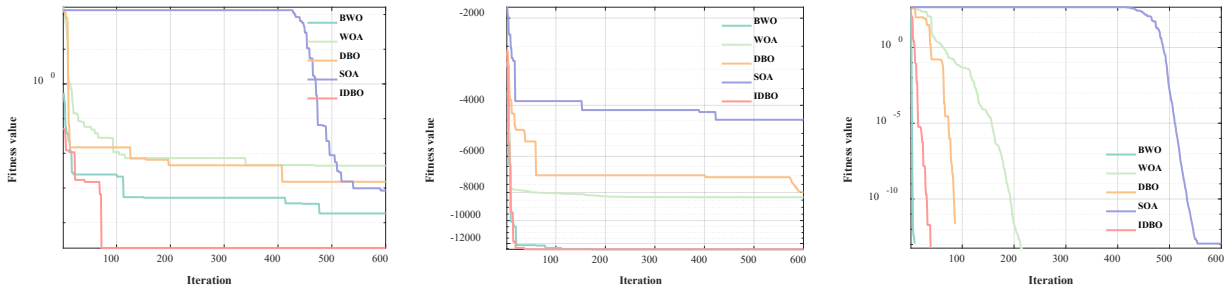

(g) F_7 (h) F_8 (i) F_9

Figure 2. Algorithm test curve

4. Experimental design and results analysis

To validate the feasibility of the IDBO algorithm in addressing the DG integration DNR problem, this study conducted experiments using the IEEE 33-bus system and systematically evaluated its reconfiguration performance through seven distinct schemes.

(i) Distribution network with DG integration and no reconfiguration.
(ii) Distribution network without DG integration and no reconfiguration.
(iii) Reconfiguration using the DBO algorithm under DG integration.
(iv) Reconfiguration using the WOA algorithm under DG integration.
(v) Reconfiguration using the SOA algorithm under DG integration.
(vi) Reconfiguration using the BWO algorithm under DG integration.
(vii) Reconfiguration using the IDBO algorithm under DG integration.

Additionally, the stability and adaptability of the algorithm in various DG scenarios were tested by altering the DG type and placement. Subsequently, in order to validate the algorithm's universality, the study further conducted tests on an IEEE 69-bus system, which demonstrates that the proposed scheme can generate feasible DNR results across distribution networks with varying architectures, thereby empirically confirming its broad applicability.

4.1. Simulation of IEEE 33-bus distribution system

To validate the effectiveness and advantages of the proposed algorithm under different distributed power source connection conditions, two comparative schemes were designed for experimentation on IEEE 33-bus system. The fundamental structure of this system comprises 33 nodes and 37 sectionalizing switches, with reference values of 10 MVA for capacity, 12.66 kV for voltage level, and 3715 kW + j2300 kVar for initial load.

Case 1: IEEE 33-bus distribution system with three DGs added

All experiments groups maintained the same DG access information, as shown in Table 4, and the algorithm are set to iterate 100 times. The system topology after integrating distributed generation is shown in Figure 3. Table 5 presents the results after reconstruction for each scheme. Analysis reveals that compared to the two scenarios before reconstruction, DG integration effectively optimizes system performance metrics, reducing network losses while enhancing voltage levels.

Furthermore, algorithmic intervention has provided better reconstruction solutions, with IDBO reducing network losses by 1.16%, 0.96%, 7.45% and 2.97% compared to DBO, WOA, SOA and BWO algorithms, respectively. Through the comparison of minimum voltage values, the applicability of IDBO in addressing DNR problems is validated. Figure 4(a-e) illustrates the node voltage magnitude distribution after reconfiguration using the DBO, WOA, SOA, BWO and IDBO, contrasting the reconfiguration outcomes of each algorithm with the voltage distribution at the inception of the distribution network with and without DG integration. By comparing the voltage distribution with and without DG integration, it is evident that DG integration effectively enhances the voltage magnitudes. The red curve in Figure 4(e) represents the voltage value of nodes after reconfiguration using IDBO algorithm, and the voltage level of each node is significantly closer to 1.

Table 4. DG information of Case 1.

Node	Type	Parameter
3	PQ	$P = 800kW$, $\cos = 0.8$
6	PQ	$P = 800kW$, $\cos = 0.9$
24	PQ	$P = 1200kW$, $\cos = 0.85$

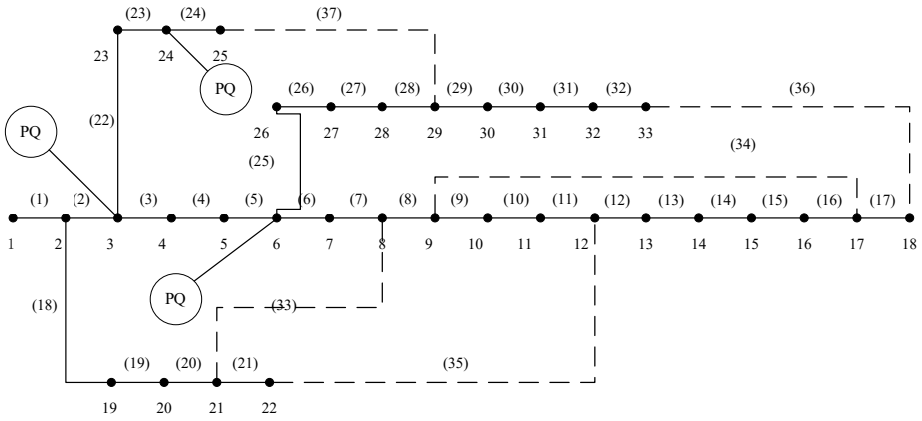

Figure 3. IEEE 33-bus structure after three DGs added.

Table 5. Reconstruction results of Case 1 in various states.

Method	Power Dissipation(kW)	Minimum Node Voltage(p.u)	Open Switches
NO DG before Operation	202.5193	0.9131	33, 34, 35, 36, 37
With DG before Operation	87.5769	0.9397	33, 34, 35, 36, 37
DBO	42.6569	0.9626	2, 14, 10, 32, 23
WOA	45.5565	0.9666	2, 14, 10, 36, 5
SOA	42.5705	0.9663	33, 14, 9, 36, 23
BWO	43.4542	0.9583	2, 14, 11, 36, 23
IDBO	42.1615	0.9678	33, 14, 9, 32, 33

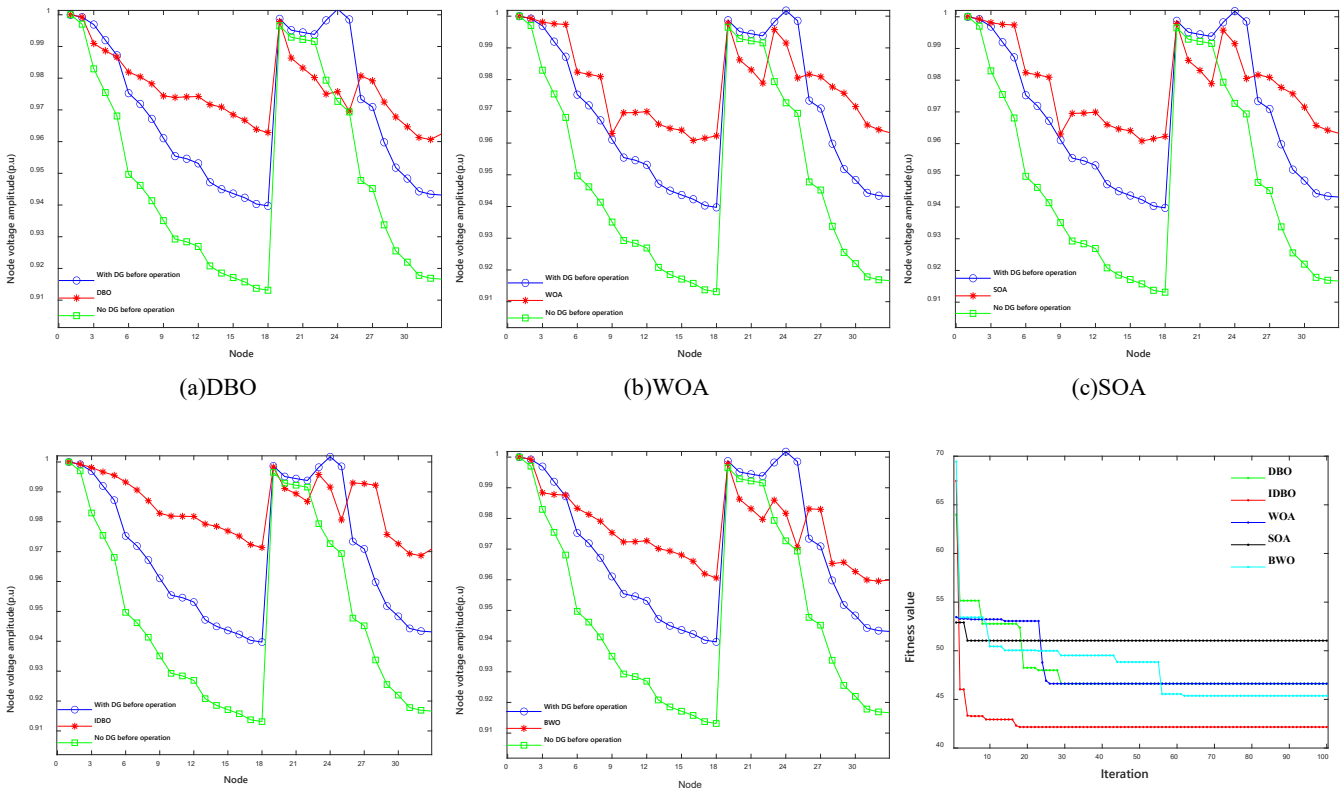

(a)DBO (b)WOA (c)SOA

(d)BWO (e)IDBO (f)Iterative curve

Figure 4. Comparison curve of Case 1 in various states: (a-e) voltage distribution after reconstruction of DBO, WOA, SOA, BWO and IDBO; (f) Iterative curve of DBO, WOA, SOA, BWO and IDBO.

Figure 4(f) illustrates the iteration curves of the five algorithms, showing that IDBO has a significantly higher convergence rate and ability to avoid local optimums compared to DBO, WOA, SOA, BWO.

Case 2: IEEE 33-bus distribution system with four DGs added

Change the location and type of DG integration while keeping the initial parameter Settings as in case 1, as detailed in Table 6. The network structure after DG access is shown in Figure 5. The results obtained from the experiment are presented in Table 7, where the optimal reconstruction scheme provided by the IDBO algorithm reduces the network loss to 34.9708 kW. With IDBO reducing network losses by 0.65%, 0.24%, 2.20%, 0.77%, compared to DBO, WOA, SOA and BWO algorithms, respectively. Minimum voltage increased to 0.9758. This is verified by the node voltage distributions shown in Figure 6 (a-e) compared to the other four schemes, the voltage distribution curves obtained by IDBO are smoother, with a higher quality of voltage and closer to the reference voltage.

Table 6. DG information of Case 2.

Node	Type	Parameter
4	PI	$P = 200kW$, $I_s = 50A$
17	PI	$P = 300kW$, $I_s = 50A$
25	PV	$P = 300kW$, $V_s = 0.98$
30	PQ	$P = 300kW$, $\cos = 0.9$

Figure 6(f) shows the iterative progress of the five algorithms. The IDBO algorithm improves the efficiency of the search process by continuously optimizing the parameters, allowing it to converge to the best solution faster than DBO, WOA, SOA and BWO.

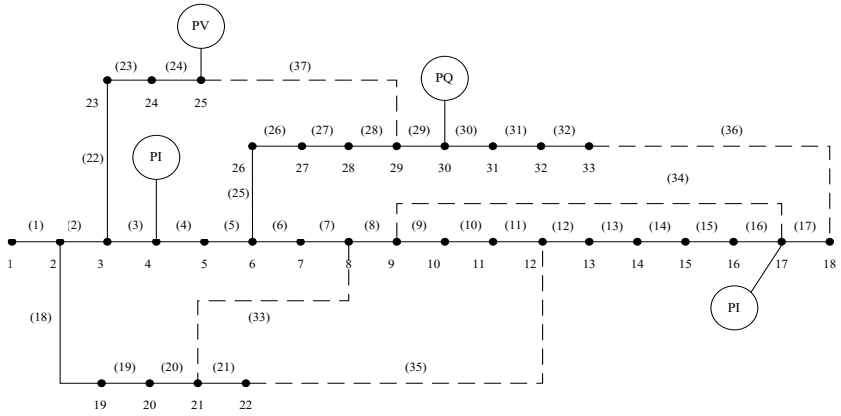

Figure 5. IEEE 33-bus structure after four DGs added

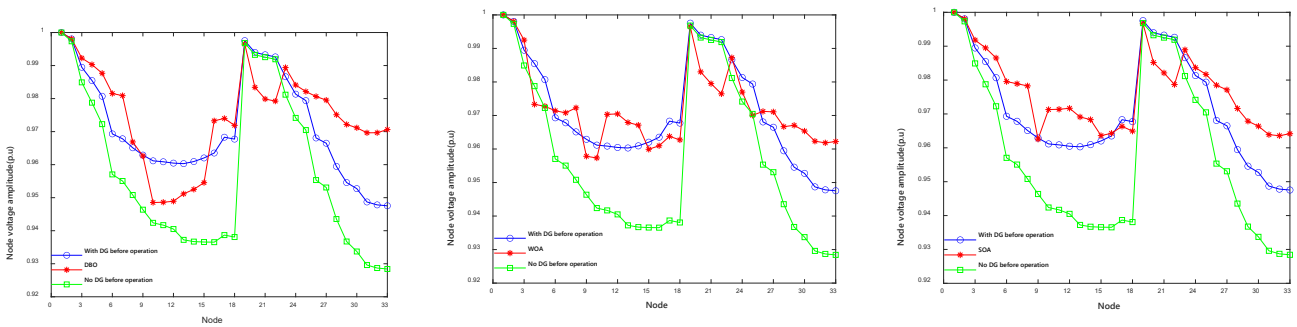

(a)DBO (b)WOA (c)SOA

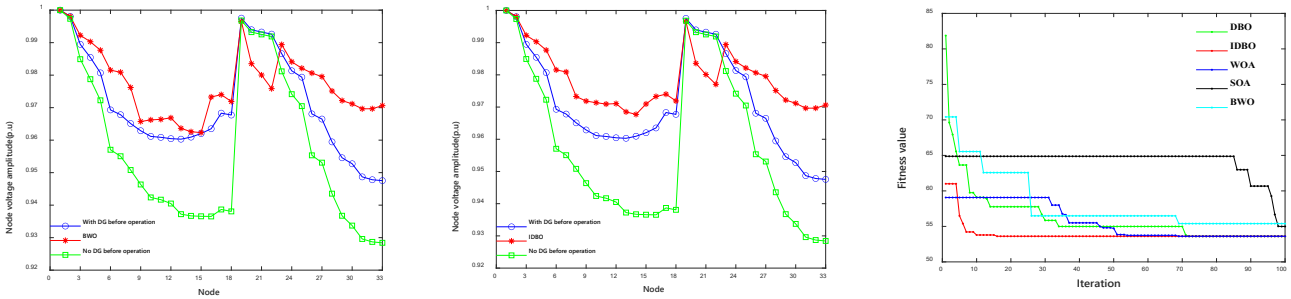

(d)BWO (e)IDBO (f)Iterative curve

Figure 6. Comparison curve of Case 2 in various states: (a-e) voltage distribution after reconstruction of DBO, WOA, SOA, BWO and IDBO; (f) Iterative curve of DBO, WOA, SOA, BWO and IDBO.

Table 7. Reconstruction results of Case 2 in various states.

Method	Power Dissipation(kW)	Minimum Node Voltage(p.u)	Parameter
NO DG before Operation	202.5193	0.9131	33, 34, 35, 36, 37
With DG before Operation	79.0475	0.9397	33, 34, 35, 36, 37
DBO	53.9619	0.9667	7, 34, 11, 15, 37
WOA	54.8174	0.9707	33, 14, 9, 16, 28
SOA	53.7414	0.9662	7, 14, 9, 15, 37
BWO	54.0299	0.9652	7, 34, 10, 15, 37
IDBO	53.6130	0.9667	7, 14, 10, 15, 37

4.2. Simulation of IEEE 69-bus distribution system

To validate the effectiveness and advantages of this algorithm under different distributed power source integration conditions, two comparative schemes were designed for testing on the IEEE 69-bus distribution system model. This model comprises 73 branches, 69 nodes, and 73 switches, with baseline capacity, voltage, and initial load set at 10 MVA, 12.66 kV, and 3802 kV + j2694.6 kvar, respectively.

Case 3: IEEE 69-bus distribution system with three DGs added

The DG information of system integration is in accord with case 1 presented also in Table 4, and the algorithm is set to iterate 100 times. The topology of the distribution network after connecting to DG is shown in Figure 7. The reconfiguration outcomes are displayed in Table 8, where the optimal reconstruction scheme provided by the IDBO algorithm reduces the net-work loss to 53.4602 kW. Compared to the different scenarios with DG reconstruction using DBO, WOA, SOA and BWO algorithms, the reduction percentages are 5.44%, 11.88%, 11.87% and 12.00%, respectively, and the minimum voltage increased to 0.9658. Figure 8(a-e) show the voltage distribution in seven scenarios. The figure under observation reveals that the voltage curve after reconfiguration with the IDBO is more uniform than the curve without DG integration and with DG integration, and is closer to the per unit value of 1 compared to the DBO, WOA, SOA, and BWO. Figure 8(f) further proves the convergence ability of IDBO.

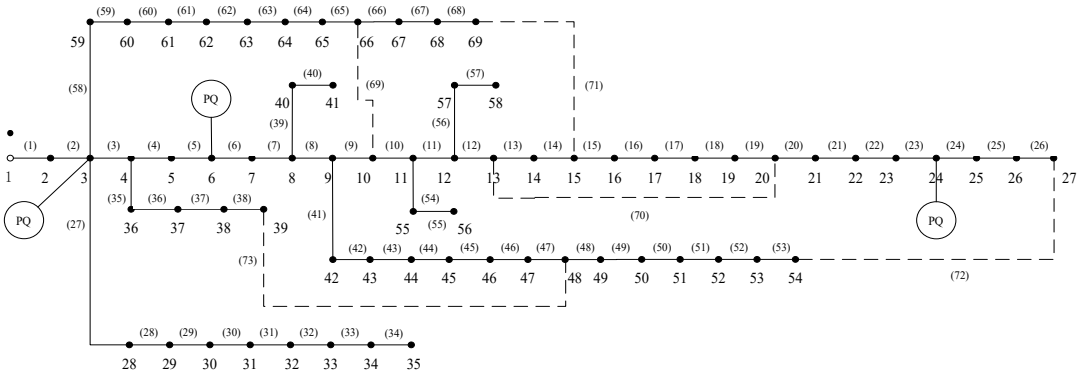

Figure 7. IEEE 69-bus structure after three DGs added

Table 8. Reconstruction results of Case 3 in various states.

Method	Power Dissipation(kW)	Minimum Node Voltage(p.u)	Parameter
NO DG before Operation	341.0235	0.8713	61, 13, 4, 43, 38
With DG before Operation	234.0108	0.8900	61, 13, 4, 43, 38
DBO	56.5352	0.9599	69, 19, 71, 11, 5
WOA	60.6652	0.9593	69, 18, 13, 11, 46
SOA	60.7538	0.9590	69, 19, 14, 11, 47
BWO	60.6625	0.9593	69, 19, 11, 13, 47
IDBO	53.4602	0.9658	69, 19, 14, 11, 4

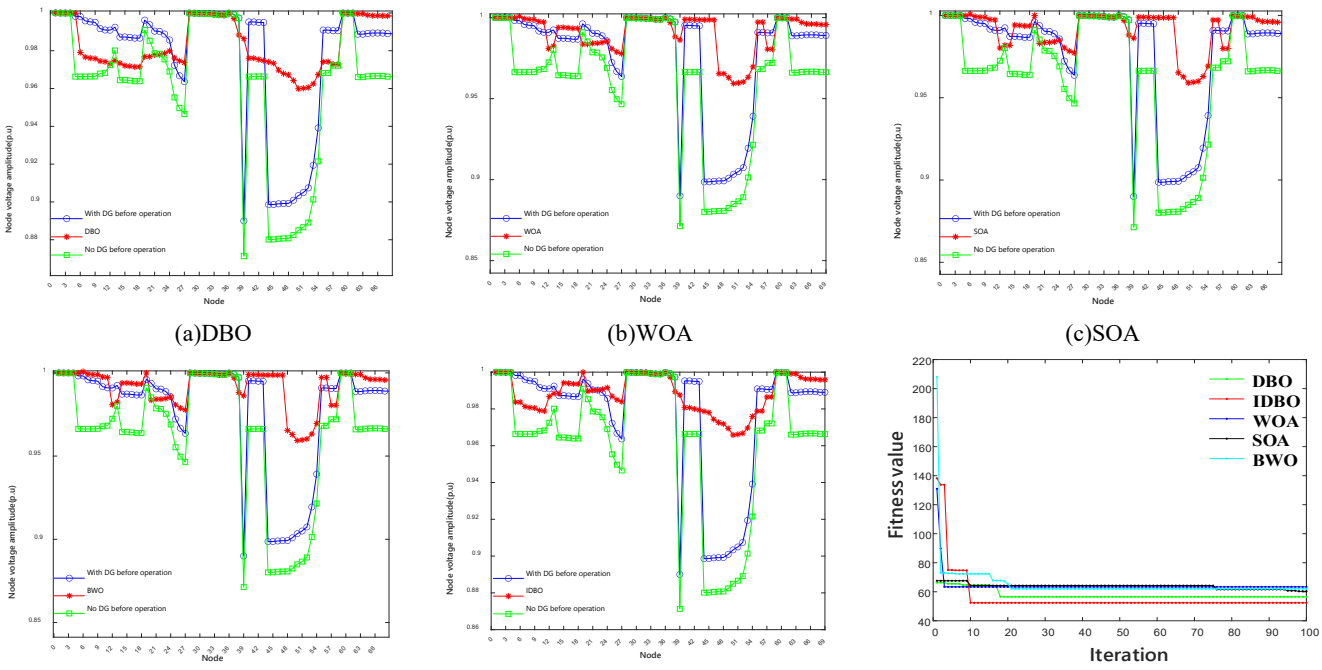

(a)DBO (b)WOA (c)SOA

(d)BWO (e)IDBO (f)Iterative curve

Figure 8. Comparison curve of Case 3 in various states: (a-e) voltage distribution after reconstruction of DBO, WOA, SOA, BWO and IDBO; (f) Iterative curve of DBO, WOA, SOA, BWO and IDBO.

Case 4: IEEE 69-bus distribution system with four DGs added

As shown in Table 9, the integrated DG information in the system was modified, and the algorithm was set to iterate 100 times. The topology of the distribution network after connecting to DG is shown in Figure 9. The reconfiguration outcomes are displayed in Table 10. The optimal reconstruction scheme provided by the IDBO algorithm reduces the network loss to 69.8845 kW. Compared with the other six scenarios before DG reconstruction without integration, before DG reconstruction with integration, and with DG reconstruction using DBO, WOA, SOA and BWO algorithms, the reduction percentages are 79.51%, 62.32%, 2.59%, 1.35%, 2.63% and 6.23%, respectively. The minimum voltage value is increased to 0.9459. Figure 10(a-e) show the node voltage amplitude curve. In Figure 10(e), the voltage amplitude curve from IDBO aligns better with the prerequisites of stable power grid function. Figure 10(f) shows the iterative comparison diagram of the five algorithms, indicating that the convergence capability of the IDBO remains superior.

Table 9. DG information of Case 4.

Node	Type	Parameter
26	PI	$P = 200kW$, $I_s = 50A$
39	PI	$P = 300kW$, $I_s = 50A$
54	PV	$P = 300kW$, $V_s = 0.98$
68	PQ	$P = 300kW$, $\cos = 0.9$

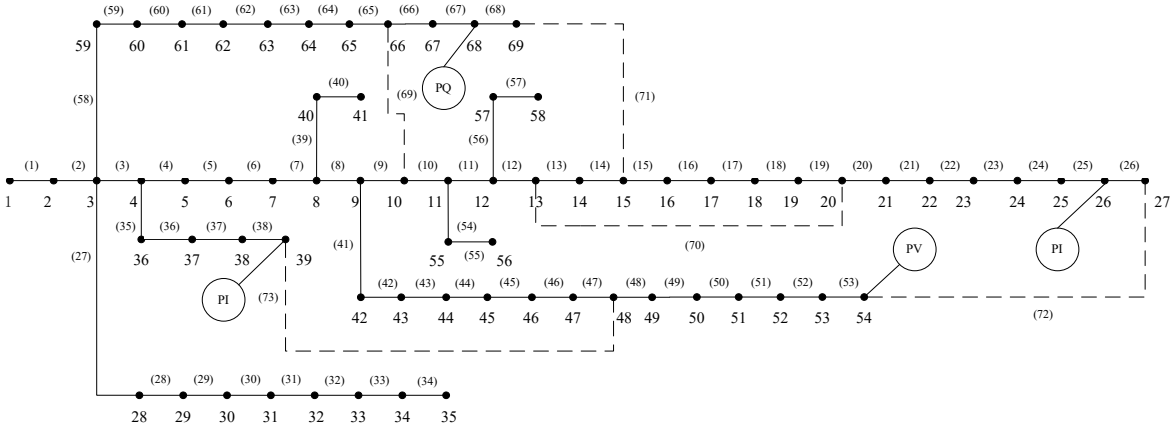

Figure 9. IEEE 69-bus structure after four DGs added.

Table 10. Reconstruction results of Case 4 in various states.

Method	Power Dissipation(kW)	Minimum Node Voltage(p.u)	Parameter
NO DG before Operation	341.0235	0.8713	61, 13, 4, 43, 38
With DG before Operation	185.4558	0.9099	61, 13, 4, 43, 38
DBO	71.7398	0.9461	69, 70, 66, 24, 46
WOA	74.5299	0.9202	10, 70, 66, 50, 46
SOA	71.7722	0.9459	64, 70, 12, 25, 44
BWO	70.8440	0.9459	10, 13, 62, 25, 44
IDBO	69.8845	0.9459	10, 70, 14, 25, 47

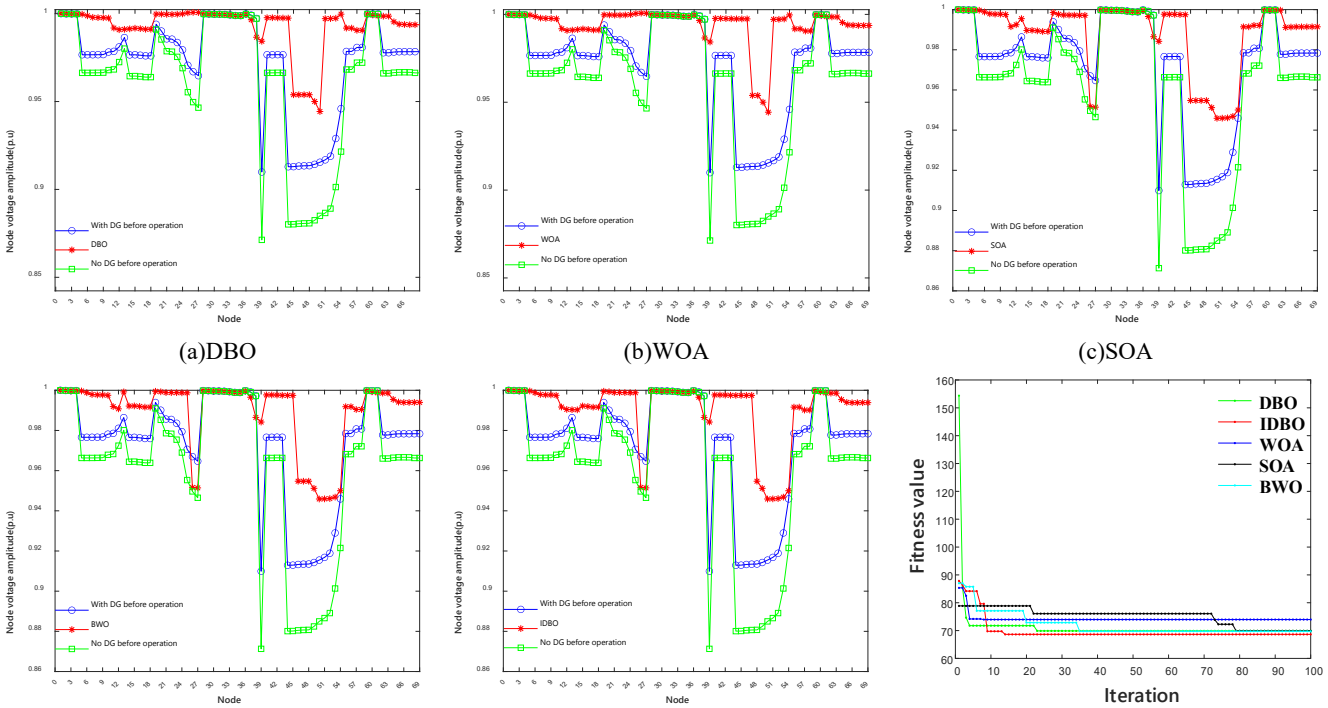

Figure 10. Comparison curve of Case 4 in various states: (a-e) voltage distribution after reconstruction of DBO, WOA, SOA, BWO and IDBO; (f) Iterative curve of DBO, WOA, SOA, BWO and IDBO.

5. Conclusion

The IDBO is proposed in this study to address complex optimization problems in distribution network reconfiguration. The algorithm integrates a variable spiral search mechanism and a Levy flight strategy to enhance global exploration capability and convergence speed. An adaptive t-distribution perturbation strategy, which adjusts with the iteration count, is introduced to strengthen local search performance. Parameters are dynamically tuned according to problem complexity, achieving an effective balance between global exploration and local exploitation. The IDBO algorithm was applied to distribution network reconfiguration and tested on two systems with different topological structures under various distributed generation integration scenarios. Simulation results demonstrate that IDBO exhibits strong adaptability, robust constraint-handling capability, and precise local search performance, highlighting its stability and versatility in providing an effective solution for complex distribution network reconfiguration problems.

Acknowledgements.

This research was supported in part by the Key Scientific Research Projects of Henan Higher Education Institutions under Grant 26A470018.

References

[1] Xiangli Chen, Yanhong Cheng, Yao Zhang, Taiyu Gu, Ye Tian. Standard demand analysis of new distribution system. Procedia Computer Science. 2024; 247: 1409-1415.

[2] BNational Energy Administration. Policy interpretation of "Guiding Opinions on High-quality Development of Distribution Network under New Situation". https://www.nea.gov.cn/. (Accessed March 1, 2024).

[3] Santos, S. F., Gough, M., Fitiwi, D. Z., Pogeira, J., Shafie-khah, M., Catalão, J. P. S.. Dynamic Distribution System Reconfiguration Considering Distributed Renewable Energy Sources and Energy Storage Systems. IEEE Systems Journal. 2022; 16 (3): 3723-3733.

[4] Badran, O., Mekhilef, S., Mokhlis, H., Dahalan, W.. Optimal reconfiguration of distribution system connected with distributed generations: A review of different methodologies. Renewable and Sustainable Energy Reviews. 2017; 73: 854-867.

[5] Wang, H.-J., Pan, J.-S., Nguyen, T.-T., Weng, S.. Distribution network reconfiguration with distributed generation based on parallel slime mould algorithm. Energy. 2022; 244: 123011.

[6] Azad-Farsani, E., Sardou, I. G., Abedini, S., Distribution Network Reconfiguration based on LMP at DG connected busses using game theory and self-adaptive FWA. Energy. 2021; 215: 119146.

[7] Rahmati, K., Taherinasab, S.. The importance of reconfiguration of the distribution network to achieve minimization of energy losses using the dragonfly algorithm. e-Prime - Advances in Electrical Engineering. Electronics and Energy. 2023; 5: 100270.

[8] Ji, X., Yin, Z., Zhang, Y., Xu, B., liu, Q.. Real-time autonomous dynamic reconfiguration based on deep learning algorithm for distribution network. Electric Power Systems Research. 2021; 195: 107132.

[9] Raut, U., Mishra, S.. An improved sine–cosine algorithm for simultaneous network reconfiguration and DG allocation in power distribution systems. Applied Soft Computing. 2020; 92: 106293.

[10] Diaaeldin, I. M., Aleem, S. H. E. A., El-Rafei, A., Abdelaziz, A. Y., Ćalasan, M.. In Optimal Network Reconfiguration and Distributed Generation Allocation using Harris Hawks Optimization. 2020 24th International Conference on Information Technology (IT), 18-22 Feb. 2020. p. 1-6.

[11] Cikan, M., Kekezoglu, B.. Comparison of metaheuristic optimization techniques including Equilibrium optimizer algorithm in power distribution network reconfiguration. Alexandria Engineering Journal. 2022; 61 (2): 991-1031.

[12] Jangdoost, A., Keypour, R., Golmohamadi, H.. Optimization of distribution network reconfiguration by a novel RCA integrated with genetic algorithm. Energy Systems. 2020; (3): 1053.

[13] Noruzi Azghandi, M., Shojaei, A. A., Toosi, S., Lotfi, H.. Optimal reconfiguration of distribution network feeders considering electrical vehicles and distributed generators. Evolutionary Intelligence. 2023; 16 (1): 49-66.

[14] Anteneh, D., Khan, B., Mahela, O. P., Alhelou, H. H., Guerrero, J. M.. Distribution network reliability enhancement and power loss reduction by optimal network reconfiguration. Computers & Electrical Engineering. 2021; 96: 107518.

[15] Shaheen, A. M.; Elsayed, A. M.; Ginidi, A. R.; El-Sehiemy, R. A.; Elattar, E., A heap-based algorithm with deeper exploitative feature for optimal allocations of distributed generations with feeder reconfiguration in power distribution networks. Knowledge-Based Systems. 2022; 241: 108269.

[16] Jafar-Nowdeh, A.; Babanezhad, M.; Arabi-Nowdeh, S.; Naderipour, A.; Kamyab, H.; Abdul-Malek, Z.; Ramachandaramurthy, V. K., Meta-heuristic matrix moth–flame algorithm for optimal reconfiguration of distribution networks and placement of solar and wind renewable sources considering reliability. Environmental Technology & Innovation. 2020; 20: 101118.

[17] Wu, Y.; Liu, J.; Wang, L.; An, Y.; Zhang, X., Distribution Network Reconfiguration Using Chaotic Particle Swarm Chicken Swarm Fusion Optimization Algorithm. Energies. 2023; 16 (20): 7185.

[18] Alqahtani, M., Marimuthu, P., Moorthy, V., Pangedaiah, B., Reddy, C. R., Kiran Kumar, M., Khalid, M.. Investigation and Minimization of Power Loss in Radial Distribution Network Using Gray Wolf Optimization. Energies. 2023; 16 (12): 4571.

[19] Xue J, Shen B.. Dung beetle optimizer: a new meta-heuristic algorithm for global optimization. The Journal of Supercomputing. 2023; 79: 7305-36.

[20] Wu Y, Wang L, Wan Z, Liu J, Fu D, An Y, Zhang X. Dynamic reconfiguration of multiobjective distribution networks considering the variation of load and DG using a novel LDEDBO algorithm. Sci Rep. 2024; 14(1): 31524.

[21] Mirjalili S, Lewis A. The whale optimization algorithm. Advances in Engineering Software. 2016; 95(5): 51-67.

[22] Mirjalili S, Moth-flame optimization algorithm: A novel nature-inspired heuristic paradigm. Knowledge Based Systems. 2015; 228- 249.

[23] Jiang M, Ma F, Zhang Y, Lv S, Pei Z, Wu G. Collaborative Scheduling Optimization of Container Port Berths and Cranes under Low-Carbon Environment. Sustainability. 2024; 16(7):2985.

[24] Zhong C, Li G, Meng Z. Beluga whale optimization: A novel nature-inspired metaheuristic algorithm. Knowledge-based systems. 2022; 251: 109215.

[25] Dhiman G, Kumar V. Seagull optimization algorithm: Theory and its applications for large-scale industrial engineering problems. Knowledge-based systems. 2019; 165: 169-196.